Earthq Eng & Eng Vib (2022) 21: 37-51 **DOI**: https://doi.org/10.1007/s11803-022-2075-6

Analytical evaluation and experimental validation on dynamic rocking behavior for shallow foundation considering structural response

Kil-Wan Ko[1†], Jeong-Gon Ha[2‡] and Dong-Soo Kim[3§]

1. *Department of Civil and Environmental Engineering, UC Berkeley, California 94720, USA*
2. *Advanced Structures and Seismic Safety Research Division, Daejeon 34057, Korea*
3. *Department of Civil and Environmental Engineering, KAIST, Daejeon 34141, Korea*

Abstract: The challenge in the practical application of rocking foundations is the estimation of its performance, particularly the rotation angle, during a strong earthquake. In this study, the dynamic rocking behavior for a shallow foundation considering structural response was evaluated through two analytical approaches: the conventional soil-foundation-structure interaction (SFSI) governing equation of a single-degree-of-freedom (SDOF) structure on a rocking shallow foundation, and the Housner rocking model (i.e., a rocking rigid block on a rigid base). Both approaches were validated with dynamic centrifuge tests. The test models consisted of a soft soil deposit, a shallow rectangular foundation, and an SDOF structure dominated by a bending behavior. A total of 11 foundation-structure systems and six seismic waves, including recorded earthquake signals and sinusoidal waves, were utilized. The results showed that the conventional SFSI equation well predicted the maximum rotation during strong earthquakes. However, this method was less accurate regarding the rotational phase information and maximum rotation of the foundation during weak earthquakes. On the other hand, although the modified Housner′s rocking model required five parameters relevant to a soil-foundation-structure system, it overestimated the maximum rotation of the foundation when compared with the results from dynamic centrifuge tests.

Keywords: soil-foundation-structure interaction; maximum rotation angle; rocking foundation; Housner rocking model; dynamic centrifuge test

1 Introduction

The necessity for a new paradigm of seismic design has been highlighted over the past three decades to handle extremely strong earthquakes (Priestley, 1993). As the available information about earthquakes has increased and the techniques for seismic analysis have advanced, force-based design has been replaced by performance-based seismic design, which is based on the performance of a structure and considers nonlinear behavior (Priestley, 2000; Priestly *et al*., 2007). However, during an unexpected strong earthquake, a nonlinear and plastic response is exhibited by not only a structure but also a soil–foundation system (Anastasopoulos *et al*., 2010). Fortunately, the approach of allowing plastic behavior of the soil-foundation system has been investigated as a replacement for prohibiting inelastic behavior of the soil-foundation system (Mergos and Kawashima, 2005; Pecker, 2006).

In particular, the rocking response among the plastic behaviors of soil-foundation systems during an earthquake have attracted research attention after Housner (1963). Various studies characterize rocking behavior through analytical, numerical, and experimental approaches (Yim *et al*., 1980; Apostolou *et al*., 2007; DeJong, 2012; Di Egidio *et al*., 2014; Vetr *et al*., 2016; Ther and Kollár, 2017). Although Housner (1963) studied the rocking response of a rigid block on a rigid base, the flexibility of a superstructure and the deformability of a support base can affect the rocking response of soil-foundation-structure systems (Pelekis *et al*., 2018). In the aspect of structural rocking, a superstructure was designed as a rigid or linear elastic superstructure. Makris and Konstantinidis (2003) introduced the rocking spectrum of a rigid block on a rigid base and compared it with the seismic response of a single-degree-of-freedom (SDOF) structure. Kavvadias *et al*. (2017) attempted to obtain a correlation between the rocking response of a rigid block and ground motion intensity measures. To evaluate the maximum rotation of a foundation-structure system, Zhang *et al*. (2019)

Correspondence to: Jeong-Gon Ha, Advanced Structures and Seismic Safety Research Division, 111, Daedeok-daero 989 Beon-gil, Yuseong-gu, Daejeon 34057, Korea
Tel: +82-42-866-6596
E-mail: jgha@kaeri.re.kr
[†]Postdoctoral Researcher; [‡]Senior Researcher; [§]Professor

Supported by: National Research Foundation of Korea (NRF) Grant funded by the Korean Government (Ministry of Science and ICT) under Grant No. 2017R1A5A1014883
Received January 8, 2021; **Accepted** November 8, 2021

proposed an equation to estimate the maximum rotation angle for a flexible superstructure on a rigid base using a simple analytical model for the representation of near-fault strong ground motions proposed by Mavroeidis and Papageorgiou (2003). However, most studies on structural rocking considered a rigid base and did not examine soil as a base.

In the geotechnical aspect, foundation rocking behavior referred to as "rocking foundation" or "rocking isolation" has been studied intensively over the past two decades (Gajan *et al*., 2005; Mergos and Kawashima, 2005; Gajan and Kutter, 2008; Deng and Kutter, 2012; Gazetas, 2015; Ko *et al*., 2018a, 2018b; Xia *et al*., 2020). It was noted that the ultimate moment capacity of the foundation can limit the structural seismic load (Anastasopoulos *et al*., 2013; Kim *et al*., 2015; Tsatsis and Anastasopoulos, 2015; Ko *et al*., 2021). The challenge in the practical application of a rocking foundation is estimating and minimizing the permanent deformation of the foundation in soil. To reduce the permanent deformation of the rocking foundation, Anastasopoulos *et al*. (2012) and Kokkali *et al*. (2015) improved the soil within a shallow depth, where plastic strain largely occurred. Allmond and Kutter (2014), Ha *et al*. (2019), and Ko *et al*. (2019) showed that the unattached pile below the rocking foundation effectively reduced the permanent deformation of the foundation as structural seismic load decreased. Most studies evaluated a rocking foundation using a rigid superstructure. Therefore, to enhance the practical application of the rocking foundation, the foundation must be evaluated using a system with a flexible superstructure on soil, which is close to practical conditions.

Several studies attempted to apply the rocking behavior of a shallow foundation to performance-based design; this was referred to as direct displacement-based design (Paolucci *et al*., 2008; Deng *et al*., 2014; Hakhamaneshi *et al*., 2016; Kutter *et al*., 2016; Khanmohammadi and Mohsenzadeh, 2018). It is crucial to determine the performance of the rocking foundation for the design method. Hence, the maximum rotation of the rocking foundation during strong earthquakes must be investigated. Anastasopoulos and Kontoroupi (2014) and Deng *et al*. (2012) obtained the correlations between the foundation rotation angle and settlement. Kourkoulis *et al*. (2012) conducted the dimensional analysis of the rocking foundation to provide an empirical equation of the toppling rotation of the system as a function of the slenderness ratio (i.e., ratio of the height of the structure to foundation length) and the vertical factor of safety. However, the actual maximum rotation caused by an earthquake is considerably less than the toppling rotation. Gajan and Kayser (2019) reported that the maximum rotation of the foundation was mainly determined by the intensity of shaking. Zhang *et al*. (2019) utilized dimensionless regression analysis to derive an equation to predict the maximum rotation of the foundation combined with a flexible structure. However, the equation is appropriate for near-fault earthquakes and a system on a rigid base.

The dynamic responses of a structure and foundation system during an earthquake were expressed as a 3×3 matrix analytical equation (i.e., three degrees of freedom: net structural response, foundation swaying, and rocking) considering soil-foundation-structure interaction (SFSI) (Kim *et al*., 2015; Ko *et al*., 2018a). The rocking response of the foundation was derived for a given earthquake signal by utilizing the analytical equation and the structural and physical properties of the foundation (i.e., stiffness and damping). However, it is difficult to precisely determine stiffness and damping because they are affected by nonlinearity and vary during strong earthquakes. Consequently, a simplified method is required to evaluate the maximum rotation of the rocking foundation considering a flexible superstructure on soil for the practical application of the foundation during a strong earthquake.

The objective of the present study is to introduce the two analytical approaches to evaluate the maximum rotation of a system with an SDOF structure on a rocking foundation during a strong earthquake using the conventional SFSI equation and Housner rocking model. The governing equation of the Housner rocking model (a rigid block on a rigid base) expresses the rotational response under horizontal ground acceleration (Zhang and Makris, 2001). Thus, first, the Housner rocking model is introduced briefly. The difference between the Housner rocking model and a rocking-dominated two degree-of-freedom (2DOF) system considering the net structural response and rocking motion of the foundation is discussed. Next, a method of evaluating the maximum rotation of the system with the SDOF superstructure on soil using the Housner rocking model is suggested. The maximum rotation from the conventional SFSI equation and the suggested method is compared and validated using the centrifuge test results of rocking foundation models. The analytical models will provide approximate solutions without using finite element methods which need significant computational cost, and provide insight into the physical mechanisms underlying the dynamic rocking foundations.

2 Housner rocking model and rocking foundation with the SDOF structure

2.1 Housner rocking model

Housner (1963) evaluated the rocking response by designing a system consisting of a rigid block on a rigid base (Fig. 1(a)). The width and height of the block are $2b$ and $2h$, respectively. The center of gravity of the block is located a distance of h above the base and a distance of b from the side of the block. The initial state of the block is rotated as a rotation angle of θ, and the block exhibits free vibration with two pivots at the end of the

side of the block. The rocking behavior of the rigid block changes the pivots from O to O' when the block hits the rigid base. The kinetic energy of the rocking motion is dissipated during impact. The reduction in energy caused by the impact, e, can be derived through the difference in the moment of momentum as follows:

$$e = \left[1 - \frac{3}{2}\sin^2\alpha\right] \tag{1}$$

where $\alpha = \tan^{-1}(b/h)$ is a damping parameter. This implies that the reduction in energy during the impact decreases with α, i.e., as a structure becomes more slender.

The rocking period of the block for the free vibration, T_R, is expressed in Housner (1963) as follows:

$$T = \frac{4}{p}\cosh^{-1}\left(\frac{1}{1-\theta/\alpha}\right) \tag{2}$$

where p is the frequency parameter of the block. For a rectangular block, $p = \sqrt{3g/4R}$, where $R = \sqrt{b^2 + h^2}$ and g = 9.8 m/s^2. This indicates that the rocking period of the block increases as the initial rotation angle of the block (θ) and the distance (R) between the center of gravity of the block and the pivot increase, as the slenderness of the block (α) decreases.

The governing equation of the rocking behavior of a rigid block on a rigid base under horizontal ground acceleration, $\ddot{u}_g$, is expressed as follows (Yim *et al.*, 1980; Makris and Roussos, 2000; Zhang and Makris, 2001; Makris and Konstantinidis, 2003):

$$\ddot{\theta}(t) = -p^2\{\sin[\alpha\,\mathrm{sgn}[\theta(t)] - \theta(t)] + \frac{\ddot{u}_g}{g}\cos[\alpha\,\mathrm{sgn}[\theta(t)] - \theta(t)]\} \tag{3}$$

Although Eq. (3) is complex, it can be solved by defining a vector-valued function, which replaces the equation by a first-order ordinary differential equation. This equation can be easily solved using the dimensions of the rigid block and horizontal ground acceleration. Hence, it is a powerful method of predicting the rocking response of the system under earthquake loading. However, the equation assumes a rigid block on a rigid base. It is required to consider soil and an SDOF structure, which allows for structural bending, to apply the equation to practical conditions.

2.2 Rocking foundation with SDOF structure

A structure considering SFSI is generally expressed as a three-degree-of-freedom system: net structural motion (u_{net}), foundation swaying motion (u_{rf}), and foundation rocking motion (u_θ). The fundamental constitutive equation for the behavior of a structure on a shallow foundation can be derived using Lagrange's equation (Craig and Kurdila, 2006). It can be expressed as Eq. (4) with a total of three degrees of freedom from the behavior due to the foundation swaying and rocking and the structural bending (Ko *et al.*, 2018a), as follows:

$$\begin{bmatrix} m_s & m_s & m_s h \\ m_s & m_s + m_f & m_s h \\ m_s h & m_s h & m_s h^2 + I_f \end{bmatrix}\begin{bmatrix} \ddot{u}_{net} \\ \ddot{u}_{rf} \\ \ddot{u}_\theta \end{bmatrix} + \begin{bmatrix} c_s & 0 & 0 \\ 0 & c_f & 0 \\ 0 & 0 & c_\theta \end{bmatrix}\begin{bmatrix} \dot{u}_{net} \\ \dot{u}_{rf} \\ \dot{u}_\theta \end{bmatrix} + \begin{bmatrix} k_s & 0 & 0 \\ 0 & k_u & 0 \\ 0 & 0 & k_\theta \end{bmatrix}\begin{bmatrix} u_{net} \\ u_{rf} \\ u_\theta \end{bmatrix} = -\begin{bmatrix} m_s \\ m_s + m_f \\ m_s h \end{bmatrix}\ddot{u}_g \tag{4}$$

where m_s is the effective mass of the structure, m_f is the mass of the foundation, I_f is the rotational moment of inertia of the foundation, h is the structural height, c_s

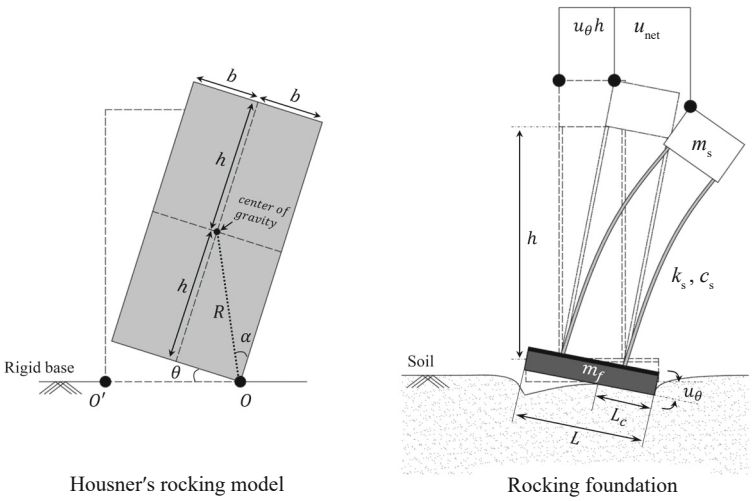

Housner's rocking model (a) Rocking foundation (b)

Fig. 1 (a) Housner rocking model: rigid block on a rigid base and (b) rocking foundation with the SDOF structure on soil

is the structural damping coefficient, c_f and c_θ are the damping coefficient of the swaying and rocking of the foundation, respectively, k_s is the effective stiffness of the structure, and k_u and k_θ are the swaying and rocking stiffness of the foundation, respectively.

A foundation-structure system with a slenderness ratio larger than one tends to rotate more than slide (Gajan and Kutter, 2009b), and this study aims to develop a simplified method to predict the maximum rotation of the rocking foundation. Hence, the dynamic behavior of the foundation–structure system corresponding to a rocking-dominated system can be described as a 2DOF system comprising net structural motion and foundation rocking motion, without foundation swaying motion (Fig. 1(b)). The conventional SFSI governing equation of the rocking foundation system without swaying can be modified as follows:

$$\begin{bmatrix} m_s & m_s h \\ m_s h & m_s h^2 + I_f \end{bmatrix}\begin{bmatrix} \ddot{u}_{net} \\ \ddot{u}_\theta \end{bmatrix} + \begin{bmatrix} c_s & 0 \\ 0 & c_\theta \end{bmatrix}\begin{bmatrix} \dot{u}_{net} \\ \dot{u}_\theta \end{bmatrix} + \begin{bmatrix} k_s & 0 \\ 0 & k_\theta \end{bmatrix}\begin{bmatrix} u_{net} \\ u_\theta \end{bmatrix} = -\begin{bmatrix} m_s \\ m_s h \end{bmatrix}\ddot{u}_g \tag{5}$$

The detailed equations utilized to calculate stiffness are summarized by Ko *et al*. (2021). If the structural and physical properties of the foundation (e.g., mass, height, stiffness, and damping) are given, the rocking response of the foundation (u_θ) for a given $\ddot{u}_g$ can be calculated by using Eq. (5) with the state space representation (Kim *et al*., 2020). The rocking response of the foundation calculated from Eq. (5) is compared with the rocking response predicted by the method using the Housner rocking model through centrifuge test models. This is described in subsequent sections.

The first row of Eq. (5) describes the horizontal structural motion. The structural seismic load, F_s, during an earthquake is obtained by arranging the first row of Eq. (5) as the following.

$$\begin{aligned} F_s &= k_s u_{net} = -m_s(\ddot{u}_{net} + \ddot{u}_\theta h + \ddot{u}_g) - c_s \dot{u}_{net} \\ &= -m_s \ddot{u}_{tot} - c_s \dot{u}_{net} \approx -m_s \ddot{u}_{tot} \end{aligned} \tag{6}$$

Here, $\ddot{u}_{tot}$ is the total horizontal structural acceleration. As the damping ratio of the structure is typically assumed to be about 5%, structural seismic load is mainly governed by $\ddot{u}_{tot}$ (Kim *et al*., 2015).

The second row of Eq. (5) presents the rocking behavior of the foundation–structure system. I_f is considerably smaller than $m_s h^2$. Thus, the term containing I_f can be excluded when the overturning moment of the foundation, M_o, is calculated. M_o is expressed using Eq. (5) as the following.

$$\begin{aligned} M_o &\approx k_\theta u_\theta = -m_s h(\ddot{u}_{net} + \ddot{u}_\theta h + \ddot{u}_g) - c_\theta \dot{u}_\theta \\ &= -m_s h \ddot{u}_{tot} - c_\theta \dot{u}_\theta \approx -m_s h \ddot{u}_{tot} \end{aligned} \tag{7}$$

Even if the moment relevant to the rotational damping of the foundation ($c_\theta \dot{u}_\theta$) influences M_o (Kim *et al*., 2015), $\ddot{u}_{tot}$ is the most crucial parameter that determines M_o (Gajan and Kutter, 2008). M_o is approximately expressed by combining Eqs. (6) and (7), as follows:

$$M_o \approx F_s h = k_s u_{net} h \approx -m_s h \ddot{u}_{tot} \tag{8}$$

As shown in Fig. 1(b), M_o induced by structural seismic load is limited by the ultimate moment capacity (M_{ult}) of the foundation, and M_{ult} for the rectangular shallow foundation is calculated as follows (Gajan *et al*., 2005; Deng and Kutter, 2012; Allmond and Kutter, 2014; Ko *et al*., 2018b):

$$\begin{aligned} M_{ult} &= V \times \Delta_r = V \times \left(\frac{L}{2} - \frac{L_C}{2}\right) \\ &= \frac{V \times L}{2}\left(1 - \frac{L_C}{L}\right) = \frac{V \times L}{2}\left(1 - \frac{A_C}{A}\right) \end{aligned} \tag{9}$$

where $V = (m_s + m_f)g$ is the total vertical load of the system, Δ_r is the rocking recentering distance, A is the foundation area, A_C is the critical contact area of the foundation (i.e., the minimum contact area of the soil-foundation interface required to resist V), L is the foundation length, and $L_C = A_C / B$ is the critical contact length of the foundation, where B is the width of the foundation. The critical contact length ratio, L / L_C, is correlated with the moment capacity, energy dissipation, and permanent settlement of the rocking foundation. The critical contact length ratio is similar to the vertical factor of safety (FS_v) of the system (Gajan and Kutter, 2008).

Due to the rocking effect, which indicates that M_o is limited by M_{ult}, the term related to the structural seismic motion, u_{net}, is limited by M_{ult}, as follows:

$$k_s u_{net} h \approx M_o \le M_{ult} = \frac{V \times L}{2}\left(1 - \frac{L_C}{L}\right) \tag{10}$$

$$\Leftrightarrow u_{net} \le \left[\frac{V \times L}{2}\left(1 - \frac{L_C}{L}\right)\right]\left(\frac{1}{k_s h}\right) \tag{11}$$

As shown by Eq. (11), the net structural displacement would converge to certain values during a strong earthquake. This relation is used to herein evaluate the maximum rotation of the rocking foundation using the Housner rocking model.

2.3 Comparison between Housner rocking model and rocking foundation with SDOF structure

Representative dynamic rotational behavior of a single lumped mass is discussed. The simplest form of rotational behavior is a simple gravity pendulum (Fig. 2(a)). The pendulum rotates freely because it is a lumped mass suspended from a pivot connected by a massless rod. The period of swing of the simple gravity pendulum is expressed as a function of the initial rotation angle and the length of the rod. However, the period is mainly governed by the length of the rod. Similarly, the rocking rigid block is expressed as a lumped mass at the center of the block, and it is referred to as an inverted pendulum (Fig. 2(b)). Its period is proportional to the distance, R. The main difference between the inverted pendulum and simple gravity pendulum is the number of pivots. The inverted pendulum loses kinematic energy when the pivot is changed to the other side of the base because of impact.

As shown in Fig. 2(c), the SDOF structure on the rocking foundation is considered as a single lumped mass at the top of the structure. This mass exhibits not only rotational behavior but also horizontal behavior (structural net motion). Even though the mass of the rocking foundation influences the rocking behavior of the entire system, which is affected by structural inertial motion (inertial interaction), the single lumped mass at the top of the structure is crucial for determining the rocking behavior of the system without the foundation mass. This implies that the dynamic behaviors of the rocking rigid block and the SDOF structure on the rocking foundation are equivalent to that of the single lumped mass with the massless rod. In this aspect, the dynamic behaviors of these two systems can be examined by investigating the dynamic behavior of the single lumped mass in detail. Note that the maximum rotation ($\theta_{\max}$) of the rocking rigid block, which is the maximum movement of the single lumped mass during an earthquake, is approximately equal to the maximum rotation of the lumped mass for the SDOF structure on the rocking foundation. This is caused by the rotation of the entire system and the net structural motion (Fig. 3) during a strong earthquake, which can make M_o converge to M_{ult}. Therefore, the relation can be expressed as follows:

$$\theta_{\max} = u_{\theta\_\max} + \theta_{\text{net\_max}} = u_{\theta\_\max} + u_{\text{net\_max}} / h \tag{12}$$

$$u_{\theta\_\max} = \theta_{\max} - \theta_{\text{net\_max}} = \theta_{\max} - u_{\text{net\_max}} / h \tag{13}$$

where $u_{\theta\_\max}$ is the maximum rotation of the rocking foundation during an earthquake, $\theta_{\text{net\_max}}$ is the maximum rotation induced by the net structural motion, and $u_{\text{net\_max}}$ is the maximum net horizontal structural displacement during an earthquake.

$\theta_{\max}$ can be easily estimated using Eq. (3) and a given earthquake time signal. Consequently, if the rocking foundation with the SDOF structure can be substituted by the Housner rocking model considering the lumped mass and $u_{\text{net\_max}}$ can be estimated, $u_{\theta\_\max}$ can be evaluated during a strong earthquake, which is the main purpose of this study (Eq. (13)). The detailed procedure for predicting $u_{\theta\_\max}$ is discussed in the following section. Table 1 compares the characteristics and parameters of the rocking rigid block and the SDOF structure on the rocking foundation to understand the fundamental differences between these models, as summarized by Makris and Konstantinidis (2003).

3 Prediction method for maximum rotation angle of rocking foundation with SDOF structure using housner rocking model

Figure 4 shows the steps of the prediction method for the maximum rotation angle of the rocking foundation with an SDOF structure during a strong earthquake. A target structure and a foundation system are converted into the SDOF structure on the rocking foundation. The converted system is assumed to be a 2DOF system: net structural response and foundation rocking. As shown in Fig. 5, the essential information of the converted target structure–foundation system for the prediction method comprises structural stiffness (k_s), structural height (h),

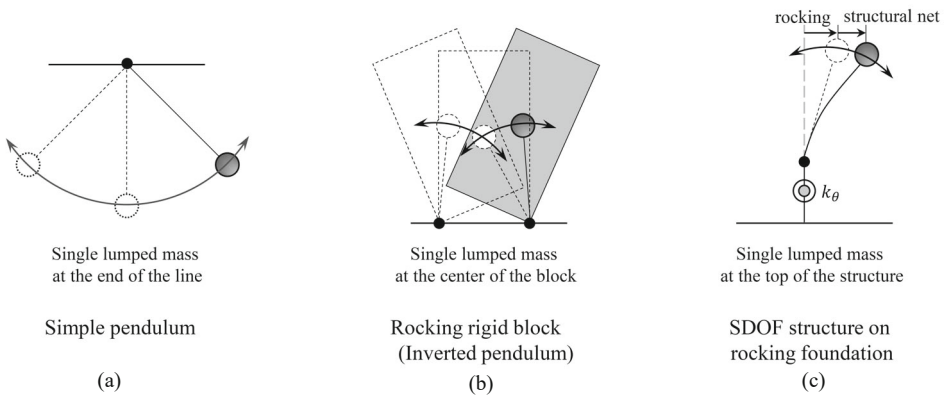

Fig. 2 Dynamic rotational behavior of single lumped mass: (a) simple pendulum, (b) rocking rigid block (inverted pendulum), and (c) SDOF structure on rocking foundation

Table 1 Comparison between Housner rocking model and rocking foundation with SDOF structure

Parameters	Housner′s rocking model	Rocking foundation with SDOF structure (2DOF system)
Superstructure	Rigid block	SDOF structure
Base condition	Rigid base	Soil (deformable base)
Degree of freedom	1 (θ)	2 (u_θ, u_{net})
Frequency parameter	$p=\sqrt{3\text{g}/4R}$	$\omega_{\text{s}}=\sqrt{k_{\text{s}}/m_{\text{s}}}$, structure $\omega_\theta=\sqrt{k_\theta/I_{\text{f}}}$, rocking
Damping parameter	$\alpha=\tan^{-1}(b/h)$	c_{s}, structure c_θ, rocking
Pivot of rotation	Edge of base	Middle point of L_{C}
Distance between center of gravity and pivot	$R=\sqrt{b^2+h^2}$	$\sqrt{b^2+\left[(L-L_{\text{C}})/2\right]^2}$
Ultimate moment	$\dfrac{V(2b)}{2}$	$\dfrac{VL}{2}\left(1-\dfrac{L_{\text{C}}}{L}\right)$

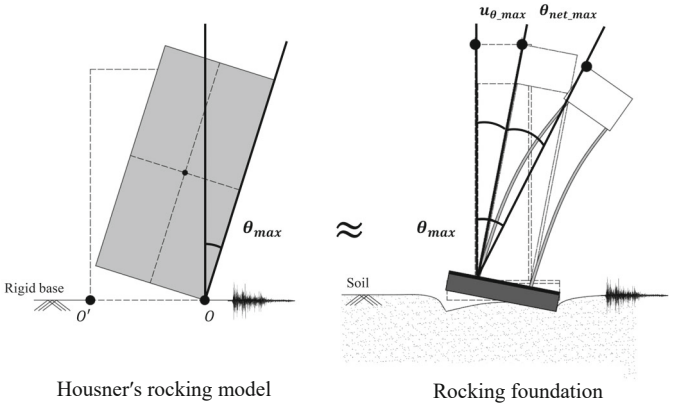

Fig. 3 Relation between maximum rotation obtained using Housner rocking model and rocking foundation with SDOF structure during strong earthquake

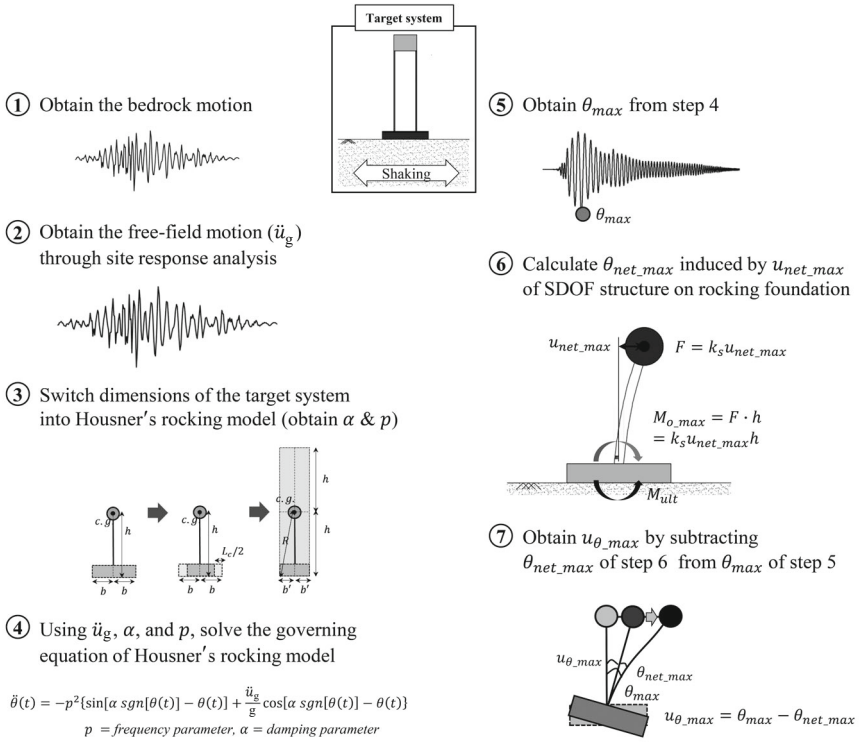

Fig. 4 Steps of prediction method for maximum rotation angle of rocking foundation with SDOF structure during a strong earthquake

foundation length ($2b = L$), the total vertical load of the system (V), and the vertical factor of safety of the system (FS_v). The process for the prediction of the maximum rotation angle of the targeted system is described as follows:

(1) The bedrock motion is obtained.

(2) Based on the bedrock motion and dynamic soil properties, the free-field motion ($\ddot{u}_g$) is determined through site response analysis. The calculated free-field motion must have sufficient ability to make the overturning moment (M_o) of the foundation converge to the ultimate moment capacity (M_{ult}) of the foundation during an earthquake.

(3) As shown in Fig. 6, the dimensions of the rocking foundation with the SDOF structure are converted to the Housner rocking model by focusing on the center of mass. When M_o converges to M_{ult}, the two pivots of the rocking foundation are located in the middle of the critical contact length (L_C). Therefore, half of the foundation length ($b = L/2$) is changed as follows:

$$b' = b - \frac{L_C}{2} = \frac{L}{2} - \frac{L_C}{2} = \frac{L}{2}\left(1 - \frac{L_C}{L}\right) = \frac{L}{2}\left(1 - \frac{1}{FS_v}\right) \quad (14)$$

where b' is the modified foundation length for the Housner rocking model. Gajan and Kutter (2008) stated that the L_C / L ratio is equal to $1/FS_v$ if the ultimate bearing pressure does not depend on the shape and size of the loaded area. Thus, b' can be expressed as a function of FS_v. This indicates that even though the targeted system is converted to the Housner rocking model, it still implies the deformable rounded soil surface that depends on FS_v. Consequently, the frequency (p) and damping parameter (α) of the converted Housner rocking model are expressed as follows:

$$p = \sqrt{3g / 4\sqrt{(b')^2 + h^2}} \quad (15)$$

$$\alpha = \tan^{-1}(b' / h) \quad (16)$$

(4) The governing equation (Eq. (3)) of the converted Housner rocking model during an earthquake is solved using $\ddot{u}_g$, p, and α, and the time history of the rotation angle of the foundation is obtained.

(5) The maximum rotation (θ_{max}) of the converted Housner rocking model is acquired from the time history of the rotation angle.

(6) Given that the foundation rocking behavior (u_θ) is in phase with the net structural response (u_{net}) (Ko *et al*., 2018a), θ_{net_max} must be removed from θ_{max} to obtain u_{θ_max}. During a strong earthquake, M_o is equal to M_{ult} due to the rocking effect. As described in Eq. (11), the maximum net horizontal structural displacement (u_{net_max}) can be expressed as follows:

$$u_{net\_max} = \left[\frac{V \times L}{2}\left(1 - \frac{L_C}{L}\right)\right]\left(\frac{1}{k_s h}\right) \quad (17)$$

Consequently, the maximum rotation θ_{net_max} induced by u_{net_max} is calculated as follows:

$$\theta_{net\_max} = \tan^{-1}(u_{net\_max} / h) = \tan^{-1}\left[\left[\frac{V \times L}{2}\left(1 - \frac{L_C}{L}\right)\right]\left(\frac{1}{k_s h}\right)\left(\frac{1}{h}\right)\right] \quad (18)$$

(7) Finally, u_{θ_max} can be obtained using θ_{max} and θ_{net_max} through Eq. (13).

The proposed method is validated using dynamic centrifuge test results and compared with the rocking behavior of the foundation calculated from Eq. (5) of the rocking-dominated 2DOF system.

4 Validation of predicited maximum rotation of rocking foundation using dynamic centrifuge tests

The dynamic centrifuge test results of previous studies (Ko *et al*., 2018a, 2021) are used to validate the analytical methods. The structure and foundation models used for the previous centrifuge tests comprise two thin

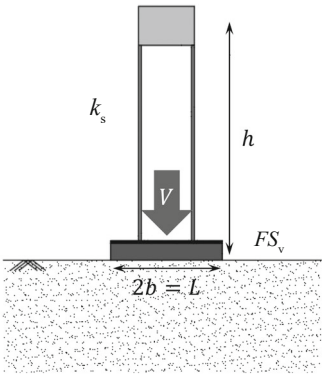

Fig. 5 Converted target structure-foundation system

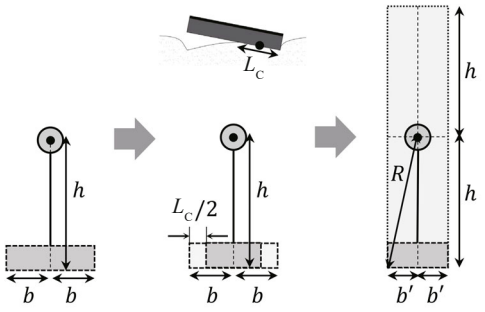

Fig. 6 Conversion of dimensions of SDOF structure on rocking foundation system to Housner rocking model

steel plates, a lumped mass on top of the structure, and a thin supporting plate that is fixed to the aluminum square foundation model with bolts, as shown in Fig. 5. It was assumed that the structural dynamic response of the model in the present study remained in the linear elastic range during strong shaking. Tables 2 and 3 summarize the properties of the test models of Ko *et al*. (2018a) and Ko *et al*. (2021), respectively. Six types of earthquakes (Ofunato, Hachinohe, Northridge, Sweep, Sine 4 Hz, Sine 2 Hz) were used and at least 30 seismic waves were inputted for each centrifuge test model. The intensities of the input motions were increased in stages from small to large. The specific descriptions of the previous centrifuge tests and models are provided in Ko *et al*. (2018a) and Ko *et al*. (2021). As stated by Gavras *et al*. (2020), the height of the structure models is considered as the height of the lumped mass. The properties of the centrifuge test models utilized by Ko *et al*. (2021) are used to predict the rocking behavior of the foundation using the method in the Housner model and the conventional SFSI governing equation (Eq. (5)) of the rocking-dominated 2DOF system. The predicted rocking behavior of the foundation is compared with the rocking behavior of the foundation measured through the dynamic centrifuge tests. Moreover, the properties of the centrifuge test models utilized by Ko *et al*. (2018a) are used to calculate the maximum rotation of the rocking foundation during an earthquake, and this rotation is compared with the rotation angle measured via the dynamic centrifuge tests.

Table 2 Properties of centrifuge test models used in a previous study (Ko *et al*., 2018a) at prototype scale

Models	ST4	ST8	ST12
Foundation length, $2b = L$ (m)	1.4	1.4	1.4
Effective mass, m_s (kg)	158000	189000	183000
Effective stifness, k_s (kN/m)	49362	11616	3656
Structural height, h (m)	1.4	2.1	2.8
Factor of safety, FS_v	11.6	11.3	11.1

4.1 Prediction of foundation rocking behavior using conventional SFSI governing equation

For a given $\ddot{u}_g$ obtained from the centrifuge free-field motion, the SFSI governing equation of the rocking-dominated 2DOF system (Eq. (5)) is expressed as a first-order differential equation using the state space representation as follows:

$$\boldsymbol{M}\begin{bmatrix}\ddot{u}_{net}\\ \ddot{u}_\theta\end{bmatrix}+\boldsymbol{C}\begin{bmatrix}\dot{u}_{net}\\ \dot{u}_\theta\end{bmatrix}+\boldsymbol{K}\begin{bmatrix}u_{net}\\ u_\theta\end{bmatrix}=-\boldsymbol{F}\ddot{u}_g \tag{19}$$

where $\boldsymbol{M}=\begin{bmatrix}m_s & m_sh\\ m_sh & m_sh^2+I_f\end{bmatrix}$, $\boldsymbol{C}=\begin{bmatrix}c_s & 0\\ 0 & c_\theta\end{bmatrix}$; $\boldsymbol{K}=\begin{bmatrix}k_s & 0\\ 0 & k_\theta\end{bmatrix}$, and $\boldsymbol{F}=\begin{bmatrix}m_s\\ m_sh\end{bmatrix}$. The net structural and foundation rotational responses are substituted as follows.

$$x_1=u_{net} \tag{20}$$

$$x_2=\dot{u}_{net} \tag{21}$$

$$x_3=u_\theta \tag{22}$$

$$x_4=\dot{u}_\theta \tag{23}$$

Equation (19) is expressed as a first-order differential equation by arranging it as follows:

$$\boldsymbol{M}\begin{bmatrix}\dot{x}_2\\ \dot{x}_4\end{bmatrix}+\boldsymbol{C}\begin{bmatrix}x_2\\ x_4\end{bmatrix}+\boldsymbol{K}\begin{bmatrix}x_1\\ x_2\end{bmatrix}=-\boldsymbol{F}\ddot{u}_g \tag{24}$$

$$\begin{bmatrix}\dot{x}_2\\ \dot{x}_4\end{bmatrix}=-\boldsymbol{M}^{-1}\boldsymbol{C}\begin{bmatrix}x_2\\ x_4\end{bmatrix}-\boldsymbol{M}^{-1}\boldsymbol{K}\begin{bmatrix}x_1\\ x_2\end{bmatrix}-\boldsymbol{M}^{-1}\boldsymbol{F}\ddot{u}_g \tag{25}$$

Table 3 Properties of centrifuge test models used in a previous study (Ko *et al*., 2021) at prototype scale

Foundation models	FND1 (Very lightly loaded system)				FND2 (Lightly loaded system)			
Foundation length, $2b = L$ (m)	2				2			
Structure models	SDOF1	SDOF2	SDOF3	SDOF4	SDOF1	SDOF2	SDOF3	SDOF4
Effective mass, m_s (kg)	2216	4176	5936	8288	2216	4176	5936	8288
Effective stifness, k_s (kN/m)	1210	1210	1210	1210	1210	1210	1210	1210
Structural height, h (m)	3.6	3.6	3.6	3.6	3.6	3.6	3.6	3.6
Total vertical load of the system, V (kN)	95.96	115.95	134.46	157.51	236.69	256.68	275.18	298.23
Factor of safety, FS_v	97.45	80.65	69.55	59.37	39.51	36.43	33.98	31.36

Finally, the response matrix, $\boldsymbol{X}$, can be expressed as a first-order differential equation:

$$\boldsymbol{X}' = \begin{bmatrix} \dot{x}_1 \\ \dot{x}_2 \\ \dot{x}_3 \\ \dot{x}_4 \end{bmatrix} = \begin{bmatrix} 0 & 1 & 0 & 0 \\ -\boldsymbol{M}^{-1}\boldsymbol{K}(1,1) & -\boldsymbol{M}^{-1}\boldsymbol{C}(1,1) & -\boldsymbol{M}^{-1}\boldsymbol{K}(1,2) & -\boldsymbol{M}^{-1}\boldsymbol{C}(1,2) \\ 0 & 0 & 0 & 1 \\ -\boldsymbol{M}^{-1}\boldsymbol{K}(2,1) & -\boldsymbol{M}^{-1}\boldsymbol{C}(2,1) & -\boldsymbol{M}^{-1}\boldsymbol{K}(2,1) & -\boldsymbol{M}^{-1}\boldsymbol{C}(2,2) \end{bmatrix} \cdot \begin{bmatrix} x_1 \\ x_2 \\ x_3 \\ x_4 \end{bmatrix} + \begin{bmatrix} 0 \\ -\boldsymbol{M}^{-1}\boldsymbol{F}(1,1) \\ 0 \\ -\boldsymbol{M}^{-1}\boldsymbol{F}(2,1) \end{bmatrix} \ddot{u}_g = \boldsymbol{A}\boldsymbol{X} + \boldsymbol{B}\ddot{u}_g \tag{26}$$

where $\boldsymbol{X} = \begin{bmatrix} x_1 \\ x_2 \\ x_3 \\ x_4 \end{bmatrix}$;

$$\boldsymbol{A} = \begin{bmatrix} 0 & 1 & 0 & 0 \\ -\boldsymbol{M}^{-1}\boldsymbol{K}(1,1) & -\boldsymbol{M}^{-1}\boldsymbol{C}(1,1) & -\boldsymbol{M}^{-1}\boldsymbol{K}(1,2) & -\boldsymbol{M}^{-1}\boldsymbol{C}(1,2) \\ 0 & 0 & 0 & 1 \\ -\boldsymbol{M}^{-1}\boldsymbol{K}(2,1) & -\boldsymbol{M}^{-1}\boldsymbol{C}(2,1) & -\boldsymbol{M}^{-1}\boldsymbol{K}(2,1) & -\boldsymbol{M}^{-1}\boldsymbol{C}(2,2) \end{bmatrix}$$

and $\boldsymbol{B} = \begin{bmatrix} 0 \\ -\boldsymbol{M}^{-1}\boldsymbol{F}(1,1) \\ 0 \\ -\boldsymbol{M}^{-1}\boldsymbol{F}(2,1) \end{bmatrix}$.

Here, $\ddot{u}_g$ is obtained as discrete time step data from the centrifuge test results. The continuous time dynamic system, which is a function of matrices $\boldsymbol{A}$ and $\boldsymbol{B}$, can be converted into a discrete time dynamic system with $\boldsymbol{A}_d$ and $\boldsymbol{B}_d$ using the continuous to discrete time (c2d) command in MATLAB. The conversion using the c2d command is explained in Kim *et al*. (2020). Given that the initial condition of $\boldsymbol{X}$ is [0; 0; 0; 0], the system response at time step (i+1) can be expressed as follows:

$$\boldsymbol{X}(i+1) = \boldsymbol{A}_d\boldsymbol{X}(i) + \boldsymbol{B}_d\ddot{u}_g(i) \tag{27}$$

During an earthquake, the shear modulus of soil decreases as shear strain increases. To reflect the nonlinear characteristics of the shear modulus for calculating foundation stiffness, FEMA 356 has suggested the effective shear modulus ratio for various site classes according to V_{s30} (Table 4) and the peak ground acceleration (PGA) at the soil surface, as shown in Fig. 7. The ground model of Ko *et al*. (2021) corresponds to an E site with a V_{s30} of less than 182 m/s.

According to the PGA at the surface, the effective shear modulus ratio is applied to calculate k_θ. The rotation of the 2DOF system is predicted using the SFSI governing equation by calculating rotational stiffness using the FEMA 356 stiffness and assuming the damping ratios of structural and foundation rotational damping as 5% which does not reflect the nonlinearity of damping for the foundation-structure system. The recorded data of the Ofunato, Hachinohe, and Northridge earthquakes are used in the centrifuge tests. The detailed calculation for the test models and the description of the earthquake signals and centrifuge tests are provided in Ko *et al*. (2021).

Figure 8 shows the time history of the measured and predicted rotational responses of the foundation with SDOF2 during weak and strong earthquakes (weak earthquake: Hachinohe, surface PGA: 0.14 g; strong earthquake: Ofunato, surface PGA: 0.66 g). The predicted time history of rotation is estimated from the conventional SFSI governing equation of the 2DOF system. Two accelerometers attached at the edge of the foundation are used to measure the dynamic rotation of the foundation during an earthquake. During a weak earthquake, the predicted rotational response is considerably larger than the measured rotational response. Furthermore, there is a phase difference between the predicted and measured rotational responses; the period of the predicted rotational response is longer than that of the measured rotational response. The absolute values of the predicted and measured maximum rotation are 0.00415 rad and

Table 4 Various site classes according to V_{s30} for effective shear modulus ratio (FEMA 356)

Site class	Site classification (V_{s30})
A	1524 m/s < V_{s30}
B	762 m/s < V_{s30} < 1524 m/s
C	365 m/s < V_{s30} < 762 m/s
D	182 m/s < V_{s30} < 365 m/s
E	V_{s30} < 182 m/s

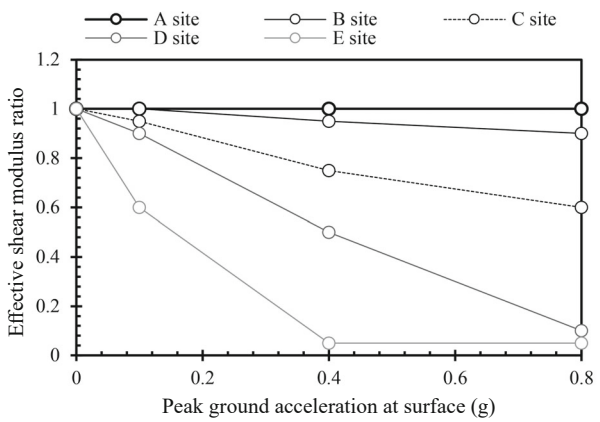

Fig. 7 Effective shear modulus ratio for various site classes and surface PGA

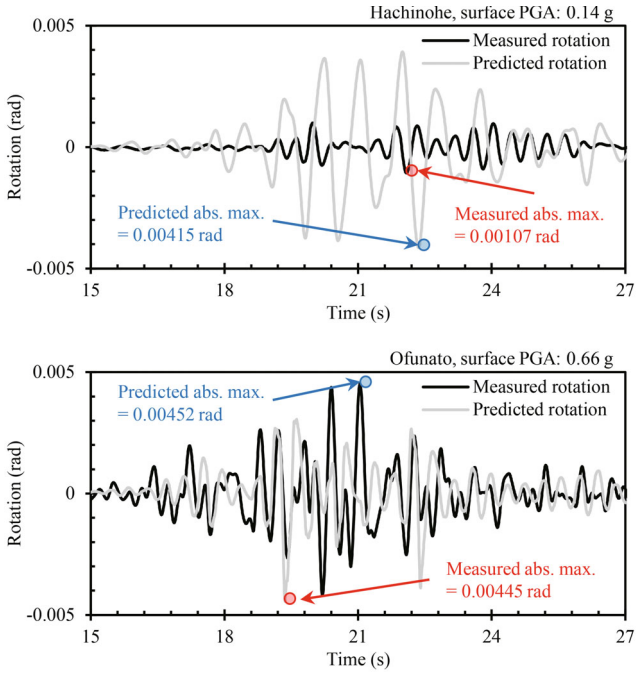

Fig. 8 Time history of measured and predicted rotational response of foundation combined with SDOF2 during weak and strong earthquakes (time history of rotational response is predicted from the conventional SFSI governing equation of the 2DOF system using centrifuge data by Ko *et al.* (2021))

0.00107 rad, respectively. The impedance functions for the foundation (frequency-dependent stiffness and damping) are not considered, and 5% damping of the foundation-structure system is used for solving the SFSI equation. Therefore, those two limitations would lead to overestimating the foundation rotation during a weak earthquake. During a strong earthquake, the phases of the predicted and measured rotation are considerably more similar compared to the weak earthquake. Moreover, since the shear modulus reduction is considered for determining the foundation stiffness, the absolute values of the predicted and measured maximum rotation are similar.

Figures 9 and 10 clearly show the trends of the predicted rotation vs. the measured rotation. Figure 9 depicts the measured and predicted maximum rotation of the foundation during the earthquake for the SDOF1, SDOF2, SDOF3, and SDOF4 testing models of Ko *et al.* (2021). The difference between the predicted and measured maximum rotation is significant during the weak earthquake (small rotation), but the difference decreases as the maximum rotation increases. In contrast, the difference decreases as the structural height of the testing model increases (i.e., a large amount of data for SDOF4 is on 1:1 line). This is because the foundation tends to exhibit more rocking compared to sliding as

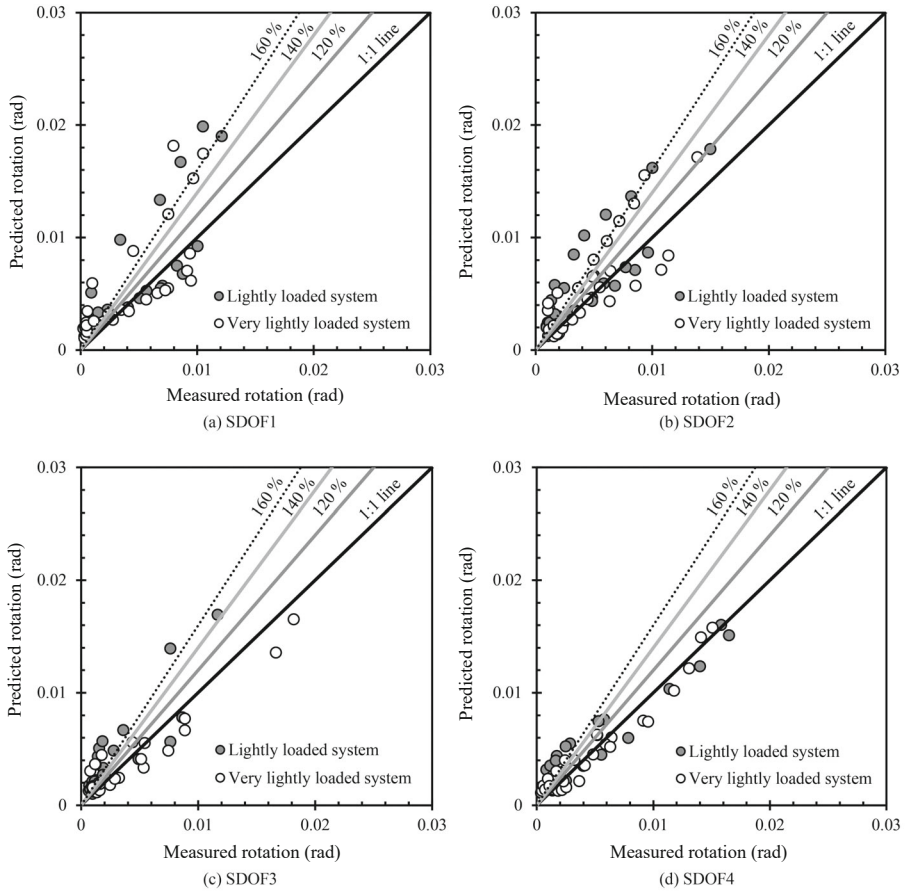

Fig. 9 Measured and predicted maximum rotation of foundation during earthquakes: (a) SDOF1; (b) SDOF2; (c) SDOF3; and (d) SDOF4 (i.e., maximum rotation is predicted from the conventional SFSI governing equation of the 2DOF system using centrifuge data by Ko *et al.* (2021))

the foundation-structure system becomes more slender. Therefore, the SFSI governing equation of the 2DOF system without sliding can accurately predict the maximum rotation of the slender foundation-structure system.

Figure 10 shows the ratio of the predicted and measured maximum rotation of the foundation vs. the PGA at the surface. When the PGA at the surface is less than 0.2 g, the values of the ratio are scattered from 0.6 to 7, but they converge to 1 as the PGA at surface increases. Although FEMA 356 suggests the effective shear modulus ratio according to PGA, which can reflect the nonlinearity of foundation stiffness, the variation in foundation stiffness within a small range of strain (weak earthquake) cannot be reflected using the effective shear modulus ratio. Consequently, the maximum rotation can be predicted through the conventional SFSI governing equation during a strong earthquake but not a weak earthquake. However, the prediction of the maximum rotation using the conventional SFSI governing equation requires considerable information about the soil-foundation-structure system, such as structural mass and stiffness, foundation mass and stiffness, and the shear modulus ratio of soil.

4.2 Prediction of foundation rocking behavior using Housner rocking model

As previously discussed, the prediction of the maximum rotation of the foundation during an earthquake using the Housner rocking model requires a few parameters of the foundation-structure system: effective structural stiffness (k_s), structural height (h), the total vertical load of the system (V), the vertical factor of safety of the system (FS_v), and foundation length (L).

Figures 11 and 12 show the measured and predicted maximum rotation of the foundation during the strong earthquake. The maximum rotation is predicted using the Housner rocking model and centrifuge data by Ko *et al*. (2021) and Ko *et al*. (2018a), respectively. The method can predict rotation using the Housner rocking model when the rocking foundation is after the yield state, which indicates that the maximum M_o during an earthquake is equal to M_{ult}. The proposed method cannot predict the maximum rotation during the weak earthquake. Accordingly, the number of data points in Fig. 11 is less than that in Fig. 9. The accuracy of the method for predicting the maximum rotation is lower than that of the conventional SFSI governing equation. The maximum rotation predicted using the method exhibits good agreement with that obtained using the centrifuge data of Ko *et al*. (2018a) (Fig. 12). As Gajan and Kutter (2008) stated that the rocking foundation can be optimized when L/L_C is close to 10, the predicted rotation and the rotation measured using the centrifuge model whose FS_v is close to 10 exhibit relatively better agreement corresponding to the models of Ko *et al*. (2018a) compared to the models of Ko *et al*. (2021).

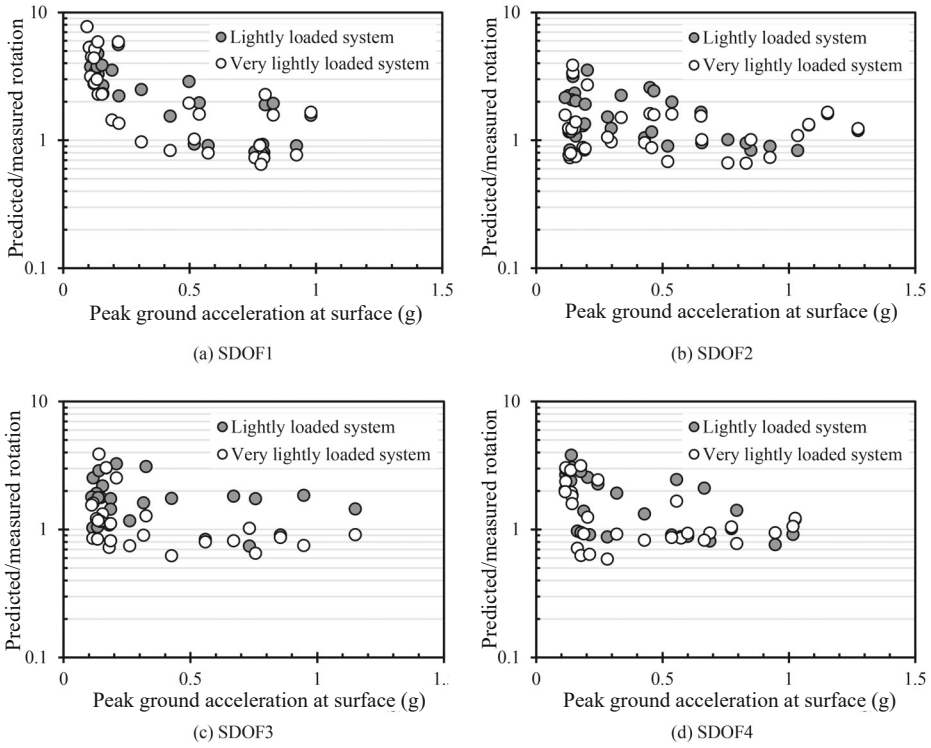

Fig. 10 Ratio of predicted and measured maximum rotation vs. peak ground acceleration at surface: (a) SDOF1; (b) SDOF2; (c) SDOF3 ; and (d) SDOF4 (i.e., maximum rotation is predicted from conventional SFSI governing equation of 2DOF system using centrifuge data by Ko *et al.* (2021))

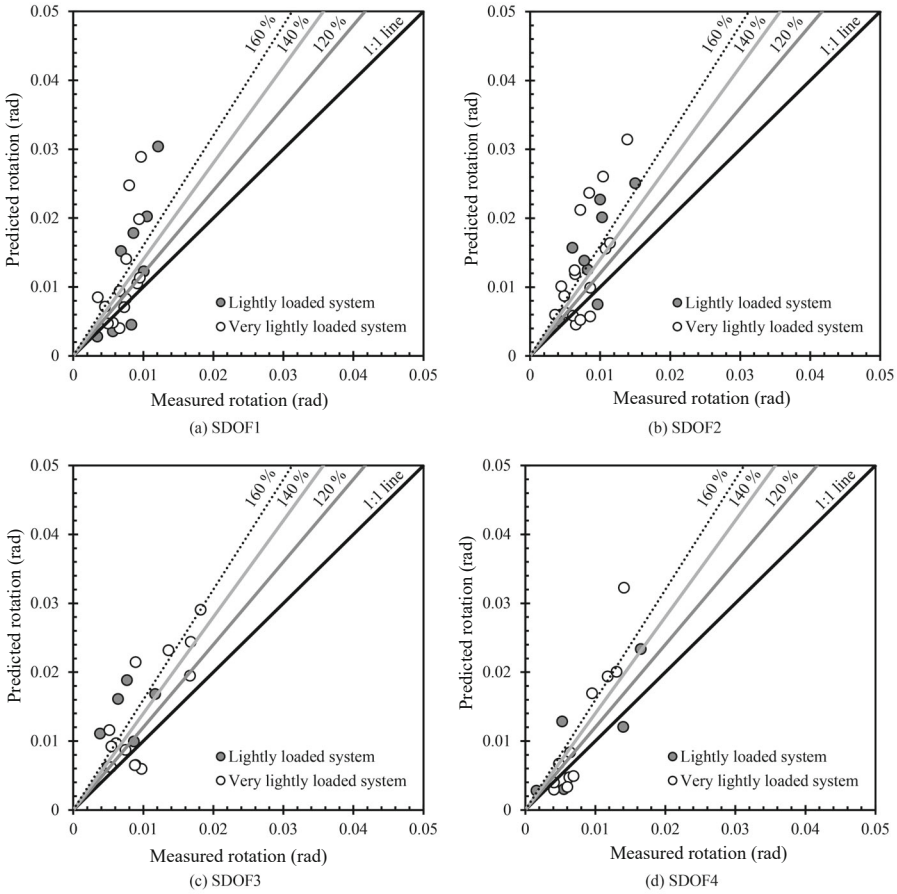

Fig. 11 Measured and predicted maximum rotation of foundation during earthquakes: (a) SDOF1; (b) SDOF2; (c) SDOF3; and (d) SDOF4 (maximum rotation is predicted using Housner rocking model and centrifuge data by Ko *et al.* (2021))

5 Conclusions and limitations

The performance of a rocking foundation, particularly rotation, during an earthquake must be evaluated to apply the foundation in practice. The analytical models for SFSI are advantageous, because these models can provide approximate solutions of dynamic response for the foundation-structure and provide insight about the SFSI effects on dynamic rocking behaviors. Therefore, to evaluate the rocking behavior of the foundation during earthquakes, two representative analytical models have been introduced: conventional SFSI model and Housner rocking model. In this study, the representative analytical models, which can both estimate the rocking behavior of the foundation, were evaluated and validated with the dynamic centrifuge tests. The conventional SFSI governing equation of the rocking-dominated 2DOF system, which can evaluate the dynamic response of foundation rotation, requires considerable information about soil-foundation-structure systems. In contrast, the modified Housner rocking model requires a few parameters: effective structural stiffness (k_s), structural height (h), total vertical load of the system (V), vertical factor of safety of the system (FS_v), and foundation length (L). However, the method using Housner model is appropriate for strong earthquakes because the yield

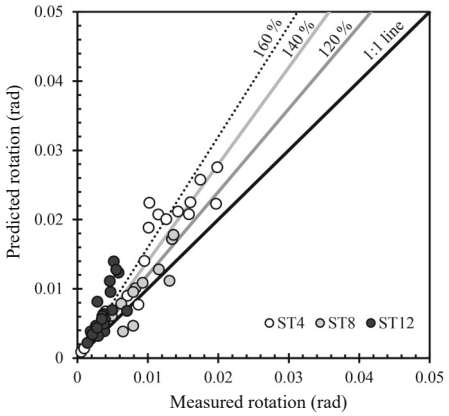

Fig. 12 Measured and predicted maximum rotation of foundation during earthquakes (maximum rotation is predicted using Housner rocking model and centrifuge data by Ko *et al.* (2018a))

state of foundation rocking behavior is reached. The main findings of this study are as follows:

(1) The conventional SFSI governing equation can predict the maximum foundation rotation during a strong earthquake. However, the predicted rotation was larger than the rotation measured from the centrifuge test results during a weak earthquake. Foundation stiffness

varies significantly within the small strain range of a weak earthquake. However, this characteristic could not be reflected by applying the effective shear modulus ratio according to the PGA at the surface.

(2) The maximum rotation predicted by the method using the Housner rocking model exhibited good agreement with the maximum rotation measured through the centrifuge tests. In addition, if the foundation-structure system was a rocking-dominated system with a large slenderness ratio, the maximum rotation predicted by the method was close to the actual maximum rotation during an earthquake.

(3) Although the accuracy of the method using the Housner model for predicting the maximum rotation was lower than that of the conventional SFSI governing equation, the Housner model was able to predict the maximum rotation using a few parameters.

The following are the limitations of this study.

(1) The foundation rocking stiffness for solving the conventional SFSI model did not reflect the frequency dependency parameters (impedance function), which could significantly affect the dynamic response of the SFSI system within the elastic regime (small strain) during weak earthquakes.

(2) Although the nonlinearity of the shear modulus ratio of soil depending on the strain level was reflected by using the effective shear modulus ratios, 5% damping was used to solve the conventional SFSI equation without considering the nonlinearity of damping.

(3) The validated structure models were lighter than the foundation models and the friction angle of the tested sand was large, so that the vertical factors of safety of the validated centrifuge test models were significantly large. In the future, to reflect practical conditions, the analytical models should be validated with the heavily loaded systems.

Acknowledgement

This work was supported by the National Research Foundation of Korea (NRF) grant funded by the Korean Government (Ministry of Science and ICT) (No. 2017R1A5A1014883).

References

Allmond JD and Kutter BL (2014), "Design Considerations for Rocking Foundations on Unattached Piles," *Journal of Geotechnical and Geoenvironmental Engineering*, **140**(10): 04014058.

Anastasopoulos I, Gazetas G, Loli M, Apostolou M and Gerolymos N (2010), "Soil Failure can be Used for Seismic Protection of Structures," *Bulletin of Earthquake Engineering*, **8**(2): 309–326.

Anastasopoulos I and Kontoroupi T (2014), "Simplified Approximate Method for Analysis of Rocking Systems Accounting for Soil Inelasticity and Foundation Uplifting," *Soil Dynamics and Earthquake Engineering*, **56**: 28–43.

Anastasopoulos I, Kourkoulis R, Gelagoti F and Papadopoulos E (2012), "Rocking Response of SDOF Systems on Shallow Improved Sand: An Experimental Study," *Soil Dynamics and Earthquake Engineering*, **40**: 15–33.

Anastasopoulos I, Loli M, Georgarakos T and Drosos V (2013), "Shaking Table Testing of Rocking—Isolated Bridge Pier on Sand," *Journal of Earthquake Engineering*, **17**(1): 1–32.

Apostolou M, Gazetas G and Garini E (2007), "Seismic Response of Slender Rigid Structures with Foundation Uplifting," *Soil Dynamics and Earthquake Engineering*, **27**(7): 642–654.

Craig JRR and Kurdila AJ (2006), *Fundamentals of Structural Dynamics*, John Wiley & Sons, Inc., New Jersey, USA.

DeJong MJ (2012), "Amplification of Rocking Due to Horizontal Ground Motion," *Earthquake Spectra*, **28**(4): 1405–1421.

Deng L and Kutter BL (2012), "Characterization of Rocking Shallow Foundations Using Centrifuge Model Tests," *Earthquake Engineering and Structural Dynamics*, **41**(5): 1043–1060.

Deng L, Kutter BL and Kunnath SK (2012), "Centrifuge Modeling of Bridge Systems Designed for Rocking Foundations," *Journal of Geotechnical and Geoenvironmental Engineering*, **138**(3): 335–344.

Deng L, Kutter BL and Kunnath SK (2014), "Seismic Design of Rocking Shallow Foundations: Displacement-Based Methodology," *Journal of Bridge Engineering*, **19**(11): 04014043.

Di Egidio A, Zulli D and Contento A (2014), "Comparison Between the Seismic Response of 2D and 3D Models of Rigid Blocks," *Earthquake Engineering and Engineering Vibration*, **13**(1): 151–162.

FEMA-356 (2000), *Prestandard and Commentary for the Seismic Rehabilitation of Buildings*, Rep., Building Seismic Safety Council (BSSC), Washington D.C., USA.

Gajan S and Kayser M (2019), "Quantification of the Influence of Subsurface Uncertainties on the Performance of Rocking Foundations During Seismic Loading," *Soil Dynamics and Earthquake Engineering*, **116**: 1–14.

Gajan S, Kutter BL, Phalen JD, Hutchinson TC and Martin GR (2005), "Centrifuge Modeling of Load-Deformation Behavior of Rocking Shallow Foundations," *Soil Dynamics and Earthquake Engineering*, **25**(7): 773–783.

Gajan S and Kutter BL (2008), "Capacity, Settlement, and Energy Dissipation of Shallow Footings Subjected to Rocking," *Journal of Geotechnical and Geoenvironmental Engineering*, **134**(8): 1129–1141.

Gajan S and Kutter BL (2009b), "Effects of

Moment-to-Shear Ratio on Combined Cyclic Load-Displacement Behavior of Shallow Foundations from Centrifuge Experiments," *Journal of Geotechnical and Geoenvironmental Engineering*, **135**(8): 1044–1055.

Gavras AG, Kutter BL, Hakhamaneshi M, Gajan S, Tsatsis A, Sharma K, Kouno T, Deng L, Anastasopoulos I and Gazetas G (2020), "Database of Rocking Shallow Foundation Performance – Dynamic Shaking," *Earthquake Spectra*, **36**(2): 960–982.

Gazetas G (2015), "4th Ishihara Lecture: Soil-Foundation-Structure Systems Beyond Conventional Seismic Failure Thresholds," *Soil Dynamics and Earthquake Engineering*, **68**: 23–39.

Ha JG, Ko KW, Jo SB, Park HJ and Kim DS (2019), "Investigation of Seismic Performances of Unconnected Pile Foundations Using Dynamic Centrifuge Tests," *Bulletin of Earthquake Engineering*, **17**(5): 2433–2458.

Hakhamaneshi M, Kutter BL, Moore M and Champion C (2016), "Validation of ASCE 41-13 Modeling Parameters and Acceptance Criteria for Rocking Shallow Foundations," *Earthquake Spectra*, **32**(2): 1121–1140.

Housner GW (1963), "The Behavior of Inverted Pendulum Structures During Earthquakes," *Bulletin of the Seismological Society of America*, **53**(2): 403–417.

Kavvadias IE, Papachatzakis GA, Bantilas KE, Vasiliadis LK and Elenas A (2017), "Rocking Spectrum Intensity Measures for Seismic Assessment of Rocking Rigid Blocks," *Soil Dynamics and Earthquake Engineering*, **101**: 116–124.

Khanmohammadi M and Mohsenzadeh V (2018), "Effects of Foundation Rocking and Uplifting on Displacement Amplification Factor," *Earthquake Engineering and Engineering Vibration*, **17**(3): 511–525.

Kim DK, Lee SH, Kim DS, Choo YW and Park HG (2015), "Rocking Effect of a Mat Foundation on the Earthquake Response of Structures," *Journal of Geotechnical and Geoenvironmental Engineering*, **141**(1): 04014085.

Kim DK, Park HG, Kim DS and Lee H (2020), "Nonlinear System Identification on Shallow Foundation Using Extended Kalman Filter," *Soil Dynamics and Earthquake Engineering*, **128**: 105857.

Ko KW, Ha JG, Park HJ and Kim DS (2018a), "Comparison Between Cyclic and Dynamic Rocking Behavior for Embedded Shallow Foundation Using Centrifuge Tests," *Bulletin of Earthquake Engineering*, **16**: 5171–5193.

Ko KW, Ha JG, Park HJ and Kim DS (2018b), "Soil Rounding Effect on Embedded Rocking Foundation via Horizontal Slow Cyclic Tests," *Journal of Geotechnical and Geoenvironmental Engineering*, **144**(3): 04018004.

Ko KW, Ha JG, Park HJ and Kim DS (2019), "Centrifuge Modeling of Improved Design for Rocking Foundation Using Short Piles," *Journal of Geotechnical and Geoenvironmental Engineering*, **145**(8): 04019031.

Ko KW, Ha JG, Park HJ and Kim DS (2021), "Investigation of Period-Lengthening Ratio for Single-Degree-of-Freedom Structures Using Dynamic Centrifuge Test," *Journal of Earthquake Engineering*, **25**(7): 1358–1380.

Kokkali P, Abdoun T and Anastasopoulos I (2015), "Centrifuge Modeling of Rocking Foundations on Improved Soil," *Journal of Geotechnical and Geoenvironmental Engineering*, **141**(10): 04015041.

Kourkoulis R, Anastasopoulos I, Gelagoti F and Kokkali P (2012), "Dimensional Analysis of SDOF Systems Rocking on Inelastic Soil," *Journal of Earthquake Engineering*, **16**(7): 995–1022.

Kutter BL, Moore M, Hakhamaneshi M and Champion C (2016), "Rationale for Shallow Foundation Rocking Provisions in ASCE 41-13," *Earthquake Spectra*, **32**(2): 1097–1119.

Makris N and Konstantinidis D (2003), "The Rocking Spectrum and the Limitations of Practical Design Methodologies," *Earthquake Engineering and Structural Dynamics*, **32**(2): 265–289.

Makris N and Roussos YS (2000), "Rocking Response of Rigid Blocks Under Near-Source Ground Motions," *Geotechnique*, **50**(3): 243–262.

Mavroeidis GP and Papageorgiou AS (2003), "A Mathematical Representation of Near-Fault Ground Motions," *Bulletin of the Seismological Society of America*, **93**(3): 1099–1131.

Mergos PE and Kawashima K (2005), "Rocking Isolation of a Typical Bridge Pier on Spread Foundation," *Journal of Earthquake Engineering*, **9**(sup2): 395–414.

Paolucci R, Shirato M and Yilmaz MT (2008), "Seismic Behaviour of Shallow Foundations: Shaking Table Experiments vs Numerical Modelling," *Earthquake Engineering and Structural Dynamics*, **37**(4): 577–595.

Pecker A (2006), "Enhanced Seismic Design of Shallow Foundations: Example of the Rion Antirion Bridge," *Proceedings of the 4th Athenian Lecture on Geotechnical Engineering*, Athens, Greece, pp.1–23.

Pelekis I, Madabhushi GSP and DeJong MJ (2018), "Seismic Performance of Buildings with Structural and Foundation Rocking in Centrifuge Testing," *Earthquake Engineering and Structural Dynamics*, **47**: 2390–2409.

Priestley MJN (1993), "Myths and Fallacies in Earthquake Engineering-Conflicts Between Design and Reality," *Bulletin of the New Zealand Society for Earthquake Engineering*, **26**(3): 329–341.

Priestley MJN (2000), "Performance Based Seismic Design," *Bulletin of the New Zealand Society for Earthquake Engineering*, **33**(3): 325–346.

Priestley MJN, Calvi GM and Kowalsky MJ (2007), *Displacement-Based Seismic Design of Structures*, IUSS Press, Pavis, Itally.

Ther T and Kollár LP (2017), "Refinement of Housner′s Model on Rocking Blocks," *Bulletin of Earthquake Engineering*, **15**(5): 2305–2319.

Tsatsis A and Anastasopoulos I (2015), "Performance of Rocking Systems on Shallow Improved Sand: Shaking Table Testing," *Frontiers in Built Environment*, **1**(9): 1–19.

Vetr MG, Nouri A R and Kalantari A (2016), "Seismic Evaluation of Rocking Structures Through Performance Assessment and Fragility Analysis," *Earthquake Engineering and Engineering Vibration*, **15**(1): 115–127.

Xia X, Wu S, Shi J, Jia J, Chen X and Ma H (2020), "Seismic Response of Rocking Isolated Railway Bridge Piers with Sacrificial Components," *Earthquake Engineering and Engineering Vibration*, **19**(4): 1005–1015.

Yim CS, Chopra AK and Penzien J (1980), "Rocking Response of Rigid Blocks to Earthquakes," *Earthquake Engineering and Structural Dynamics*, **8**(6): 565–587.

Zhang J and Makris N (2001), "Rocking Response of Free-Standing Blocks Under Cycloidal Pulses," *Journal of Engineering Mechanics*, **127**(5): 473–483.

Zhang J, Xie Y and Wu G (2019), "Seismic Responses of Bridges with Rocking Column-Foundation: A Dimensionless Regression Analysis," *Earthquake Engineering and Structural Dynamics*, **48**(1): 152–170.